



## RESEARCH ARTICLE

10.1002/2014JC010485

## Key Points:

- The North Sea can be delineated into five distinct stratification regimes
- These regimes show remarkably stable spatial occurrence
- 29% of the area defies classification due to high interannual variability

## Supporting Information:

- Supporting Information S1
- Movie S1

## Correspondence to:

S. van Leeuwen,  
sonja.vanleeuwen@cefas.co.uk

## Citation:

van Leeuwen, S., P. Tett, D. Mills, and J. van der Molen (2015), Stratified and nonstratified areas in the North Sea: Long-term variability and biological and policy implications, *J. Geophys. Res. Oceans*, 120, doi:10.1002/2014JC010485.

Received 3 OCT 2014

Accepted 9 JUN 2015

Accepted article online 12 JUN 2015

## Stratified and nonstratified areas in the North Sea: Long-term variability and biological and policy implications

Sonja van Leeuwen<sup>1</sup>, Paul Tett<sup>2</sup>, David Mills<sup>1</sup>, and Johan van der Molen<sup>1</sup>
<sup>1</sup>Centre for Environment, Fisheries and Aquaculture Science, Environment and Ecosystems Division, Lowestoft, UK,

<sup>2</sup>Scottish Association for Marine Science, Scottish Marine Institute, Department of Microbial and Molecular Biology, Oban, Argyll, UK

**Abstract** The European Unions' Marine Strategy Framework Directive aims to limit anthropogenic influences in the marine environment. But marine ecosystems are characterized by high variability, and it is not trivial to define its natural state. Here, we use the physical environment as a basis for marine classification, as it determines the conditions in which organisms must operate to survive and thrive locally. We present a delineation of the North Sea into five distinct regimes, based on multidecadal stratification characteristics. Results are based on a 51 year simulation of the region using the coupled hydrobiogeochemical model GETM-ERSEM-BFM. The five identified regimes are: permanently stratified, seasonally stratified, intermittently stratified, permanently mixed, and Region Of Freshwater Influence (ROFI). The areas characterized by these regimes show some interannual variation in geographical coverage, but are overall remarkable stable features within the North Sea. Results also show that 29% of North Sea waters fail to classify as one of the defined stratification regimes, due to high interannual variability. Biological characteristics of these regimes differ from diatom-based food webs in areas with prolonged stratification to *Phaeocystis*-dominated food webs in areas experiencing short-lived or no stratification. The spatial stability of the identified regimes indicates that carefully selected monitoring locations can be used to represent a substantive area of the North Sea.

## 1. Introduction

Over the past decades, increased understanding of physical processes and increased computational power have led to the progression from simple hydrodynamic models [e.g., *Pingree and Griffiths*, 1978,  $M_2$  tidal model] to multidecadal hindcasts and forecasts of entire shelf seas [*Holt et al.*, 2003; *Siddorn et al.*, 2007; *Kühn et al.*, 2010; *Wakelin et al.*, 2012; *van Leeuwen et al.*, 2013], including frontal regions, coastal currents, density stratification, and ROFI (Region Of Freshwater Influence) areas. The same progression is noticeable in the marine biological sciences, which started with plankton as indicators of water masses, followed by the understanding that phytoplankters especially related more to vertical processes [*Margalef*, 1978], and, by way of *Legendre and Rassoulzadegan* [1995, 1996] coming to see lifeforms of marine primary producers in relation to the (more terrestrially oriented) concept of biomes [*Tett et al.*, 2007]. *Smith* [1992] and *Ricklefs et al.* [2007] define a biome as a community resulting from a dominant lifeform of primary producer, in turn determined by environmental conditions. This definition can be applied both to terrestrial and marine environments.

Within the marine environment, the EU Marine Strategy Framework Directive (MSFD) aims to "achieve or maintain Good Environmental Status" (GES) in European seas. The directive (article 3.5) defines GES as meaning "the environmental status of marine waters where these provide ecologically diverse and dynamic oceans and seas which are clean, healthy and productive within their intrinsic conditions . . ." This raises the question of what the intrinsic conditions actually are: what sort of marine ecosystem would occur (in the absence of human interference) in a given physical environment? In this article, we begin to apply the conceptual model that the physical regime (of short-term/ seasonal/ permanent stratified conditions/ mixed conditions) selects for a particular lifeform of primary producer, and thus for the food web/biological community.

This article begins the application by mapping physical regimes in the North Sea, and considering the effects of these regimes on pelagic primary producers. As a basis we use the most important large-scale physical feature in shallow shelf seas: density stratification of the water column, which occurs when

© 2015. The Authors.

This is an open access article under the terms of the Creative Commons Attribution License, which permits use, distribution and reproduction in any medium, provided the original work is properly cited.

buoyancy of surface waters (through fresh-water input or solar heating) prevails over turbulence and vertical mixing (through wind and tides), and which limits vertical exchange across the pycnocline. The aim of this paper is therefore to identify the present density stratification regimes in the North Sea and the areas in which they occur, thus allowing for a delineation of areas within the North Sea for the identification of eco-hydrodynamic regions. These regions can then be used as a basis for marine spatial planning and ecological assessment of GES. To this end, we will analyze 51 years of simulated hindcast data of the North Sea. The use of modeled results ensures a consistent spatial and temporal coverage that observations cannot match.

## 2. Marine Biomes

### 2.1. The Biome Concept

For terrestrial ecologists, the concept of biome as an organized community of biota goes back to *Clements* [1916, 1936]. Modern definitions are given by *Odum and Barrett* [2005]; *Ricklefs et al.* [2007]; and *Smith* [1992]. The essence of these definitions is the idea of a biome as a category of ecosystem characterized by the lifeform of its primary producers. This lifeform is that adapting the producers to the prevailing environmental conditions, and is what shapes the remainder of the organization and functioning of the ecosystem. In the case of marine ecosystems, the defining conditions are those involving water depth and transparency, and stratification regime [Tett et al., 2007]. We are concerned in this paper with, in general, continental shelf waters that are too deep for significant phytobenthic growth, and, in particular, with the waters of the North Sea in which the phytoplankton is the chief community of primary producers. We expect differences in primary producers to result in differences in the rest of the pelagic food web, but do not investigate such consequences in this paper.

### 2.2. Continental Shelf Primary Producers

Unlike in terrestrial and shallow-water marine ecosystems, pelagic phytoplankters, the characteristic lifeform of primary producer in offshore waters (more than 12 nautical miles from the coast), are not rooted in or attached to the seabed. Thus, early attempts at understanding the reasons for characteristic marine floras and faunas tried to relate these to mobile water masses, leading to discrimination based on “plankton indicators” [Hardy, 1956; Russell, 1939]. However, *Margalef* [1978] placed the focus on the relationship between phytoplankters and vertical processes in aquatic environment, seeing the “different lifeforms observed in phytoplankton . . . as adaptations to survival in an unstable and turbulent environment,” and suggesting that different kinds of phytoplankter—in particular (in the sea), diatoms and dinoflagellates, would tend to be most abundant in certain sorts of environment: diatoms (which tend to sink) for example flourishing in more energetic waters and dinoflagellates (able to swim) in more stratified conditions (see also *van Haren et al.* [1998]). These ideas, based on the interaction between the size, shape, and movement capabilities of different kinds of phytoplankters, were further developed for freshwaters by *Reynolds* [1989] [see also *Reynolds et al.*, 2002] and for the sea by *Smayda and Reynolds* [2001]. Applied to additional lifeforms, they underpin much modern thinking in biological oceanography: e.g., *LeQuéré et al.* [2005].

In the case of terrestrial biomes, characteristic dominant lifeforms such as trees are long-lived, and are often accompanied by other producer lifeforms exemplified by the shrubs and herbs that form lower layers in woodland. Marine pelagic producers are short-lived, and seasonal successions, such as that from diatoms dominating a spring bloom to flagellates and dinoflagellates making up most of the biomass during summer, are typical of the continental shelf phytoplankton of temperate latitudes, a consequence of the strong seasonal cycle of the physical forcing. In our marine application of the biome concept, we consider the climatological seasonal cycle as a crucial part of phytoplankton community structure.

### 2.3. Underlying Physical Conditions

Ideas about the nature of shelf seas changed markedly in the 1970s as a result of the discovery of tidal mixing fronts [Simpson and Hunter, 1974], which seemed to exert a profound influence on phytoplankton [Pingree et al., 1975]. This led to a decade of work exploring the relationship between vertical mixing and plankton (reviewed in Tett and Edwards [1984]). As part of their studies, *Pingree and Griffiths* [1978] calculated the stratification parameter  $S = \log_{10} \left( \frac{h[m]}{C_D \cdot \langle |u[m/s]|^3 \rangle} \right)$  (based on *Simpson and Hunter* [1974]  $h/u_s^2$ ) for a grid of points on the N-W European continental shelf around Britain and Ireland (with  $h$  representing local water depth and  $C_D$  the bottom drag coefficient). Velocities  $u$  were predicted by a model of the  $M_2$  tide. The

critical value of  $S$  (1.5) predicting the position of tidal frontal boundaries was calibrated from infrared satellite imagery and ship measurements of sea surface temperature. They were then able to map the shelf sea into (1) regions that are well mixed throughout the year ( $S < 1$ ), (2) (tidal) frontal regions ( $1 < S < 2$ ), and (3) regions that are (thermally) stratified during summer months. As they pointed out, the frontal zones that separate the mixed and seasonally stratified regions, “represent important physical, biological, and chemical boundaries.”

This map, and the concepts it embodied, has subsequently been highly influential in guiding studies of shelf seas. The “ $h/u^3$ ” theory, on which it is based, assumes a balance between potential-energy creating inputs of thermal buoyancy and kinetic-energy creating inputs through wind and tidal stirring and internal wave breaking. This balance, or lack of it, determines the vertical diapycnal exchange, allowing for the onset of stratification when turbulence levels reduce sufficiently in spring [van Haren *et al.*, 1999]. Blooms can start before this onset in relatively shallow areas like the Oyster Grounds (45 m) if conditions are right and high turbulence levels keep diatoms suspended in the euphotic zone. This is followed by diatom sinking and onset of stratification when turbulence levels subside sufficiently [van Haren *et al.*, 1998]. In contrast, in deeper areas like the Fladen Ground (90–170 m) spring bloom dynamics are triggered by the establishment of vertical thermal stratified conditions [Williams and Lindley, 1980]. In some parts of shelf seas, however, locally and advected inputs of freshwater buoyancy are significant. These can create or intensify existing density stratification, or lengthen the part of the year during which the water column is stratified, as for examples in the Firth of Clyde in Scotland [Simpson and Rippeth, 1993] or the Norwegian Coastal Current [Mork, 1981]. In shallow waters close to the outflows of large rivers, variable freshwater discharges, and wind-driven movements of estuarine plumes, result in rapidly alternating periods of stratification and mixing. These regions have been named Regions of Freshwater Influence (ROFI's) [Simpson, 1997; Verspecht *et al.*, 2009].

## 2.4. Approach

The development of hydrodynamic models such as GETM, which take into account the processes just described, allows an updated account of the water column dynamics in the North Sea to provide a basis for improved understanding of phytoplankton ecology. We have used the ecosystem model ERSEM-BFM to explore the effects of stratification regime on the floristic composition of the phytoplankton. van der Molen *et al.* [2013] has shown that this model is capable of reproducing the different characteristics of stratification onset and biological response mentioned above: diatom bloom before stratification onset at the Oyster Grounds (followed by diatom sinking when surface and bottom temperatures start to diverge) and diatom bloom triggered by stratification at a site north-west of the Dogger Bank (80 m depth).

Biomes are held to be categories that map to discrete (dynamical) stable states of ecosystems. Although the physical state of the North Sea varies continuously in space, it will be useful for practical purposes to identify simulated regimes as far as possible with the categories already mentioned, of seasonally stratified, mixed and ROFI. We look for such categorization in the results of the model, as reported in section 4 and then in section 5 consider how far it applies to the primary producer lifeforms simulated by the ecosystem model.

## 3. The Applied Ecosystem Model

The model used to simulate the marine ecosystem in the North Sea is the coupled hydrobiogeochemical model GETM-ERSEM-BFM.

### 3.1. Physical Model

The hydrodynamic General Estuarine Transport Model (GETM) is an open source model available from [www.getm.eu](http://www.getm.eu) and described in detail in Burchard and Bolding [2002]; Stips *et al.* [2004]. The GETM model applies the General Ocean Turbulence Model (GOTM) for description of the vertical processes (for details see [www.gotm.net](http://www.gotm.net)). GETM is a fully baroclinic model including sea surface elevations, currents, drying and flooding of land cells, temperature, and salinity. General vertical coordinates were applied together with a Cartesian, staggered C-grid in the horizontal. The resolution of 6 nm is similar to that of Pingree and Griffiths [1978] (5 nautical mile). Progress since 1978 has lead to many differences of the applied model with respect to Pingree and Griffiths [1978], of which the most important ones are the advanced mathematical solving

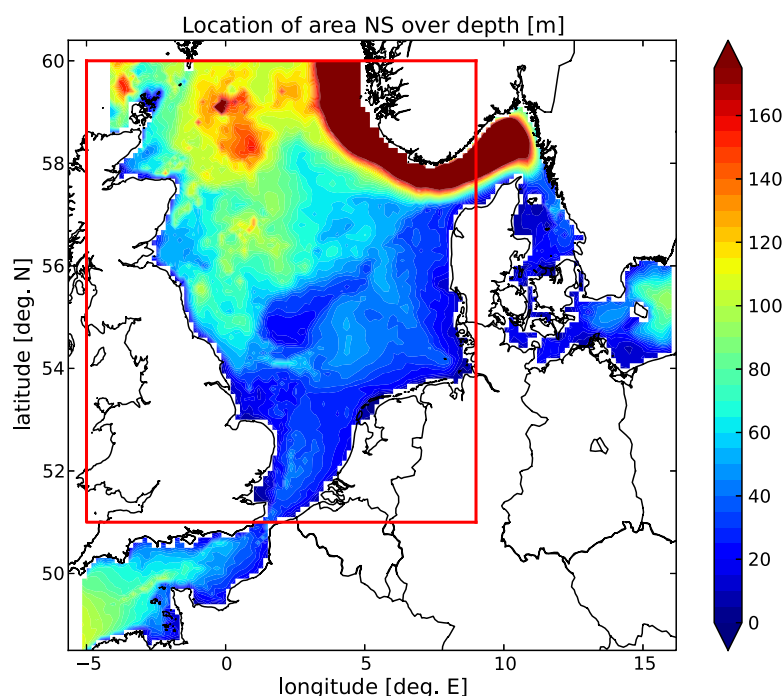


**Figure 1.** Applied model domain and bathymetry, and definition of the North Sea area.

scheme, the inclusion of diffusion, representation of vertical processes and forcing by all major tidal components. A second order turbulent closure method (EASM with weak equilibrium) was applied. Internal waves are not expected to be represented well in the model because of the limited vertical resolution and the associated numerical diffusion. This could be improved by introducing vertical adaptive coordinates [Hofmeister *et al.*, 2010, 2011]. Note that internal wave breaking can cause short-lived injections of nutrients to the upper mixed layer, leading to short summer blooms or autumn blooms [van Haren *et al.*, 1999]. This mechanism is not expected to be reproduced by the model.

The applied model domain and bathymetry (provided by NOOS; [www.noos.cc](http://www.noos.cc)) are shown in Figure 1. Within the model domain, the North Sea is defined as the area between 51.0 and 60.0° N and −5.0 to 9.0° E, covering a total wet area of 688,288.5 km<sup>2</sup>.

### 3.2. Biological Model

The biogeochemical model ERSEM-BFM has been developed from the original ERSEM and BFM codes in a joint effort by Cefas ([www.cefas.gov.uk](http://www.cefas.gov.uk)) and NIOZ ([www.nioz.nl](http://www.nioz.nl)) research institutes, with the specific aim to improve benthic-pelagic coupling in ecosystem models to better represent shallow shelf seas. For more details on the original ERSEM model see Baretta *et al.* [1995], the coupled GETM-ERSEM-BFM model is described in more detail in Lenhart *et al.* [2010] (includes general validation results), van Leeuwen *et al.* [2013] (includes validation results for vertical distribution of phytoplankton), and [van der Molen *et al.*, 2013] (includes detailed validation results for pelagic-benthic exchange). The model currently comprises six phytoplankton function groups, five zooplankton functional groups, and five benthic groups, and includes benthic and pelagic aerobic and anaerobic bacteria (including nitrifying archaea). Organisms in ERSEM and therefore in ERSEM-BFM have internally varying nutrient ratios (i.e., are not bound by the Redfield ratio). Improvements in ERSEM-BFM also include the production of TEP (transparent exopolymer particles) under nutrient stressed conditions by diatoms and Phaeocystis colonies. Relevant features of the six phytoplankton groups are shown in Table 1. Phytoplankton in ERSEM-BFM cannot “swim,” i.e., actively control its vertical movement. Instead, advective and diffusive processes move phytoplankton around, combined with increased sinking due to TEP production (TEP causes all phytoplankton groups to sink if present). Phytoplankton size determines its ability to take up nutrients (i.e., surface/volume ratio), resulting in the ability of small phytoplankton like picophytoplankton to exist in nutrient-poor conditions, whereas larger species like

**Table 1.** Relevant Details of the Phytoplankton Functional Groups in the Applied Version of ERSEM-BFM (+ Means a Process Is Included)<sup>a</sup>

Group	Si Uptake	TEP Prod.	ESD ( $\mu\text{m}$ )	Div. (1/d)
Diatoms	+	+	20–200	1
Small diatoms	+	+	2–20	1
Flagellates	-	-	2–20	1
Picophytoplankton	-	-	0.2–2	2
Dinoflagellates	-	-	> 100	1
Phaeocystis	-	+	Colonies	2

<sup>a</sup>ESD refers to the equivalent spherical diameter of phytoplankton cells. Division times per day for *Phaeocystis* refers to organisms inside a colony.

(dino)flagellates can only thrive in nutrient richer surroundings. This results in an additional vertical distribution of the functional groups related to nutrient profiles.

Hydrodynamic and biogeochemical model results of the GETM-ERSEM-BFM code can also be viewed at [www.nioz.nl/northsea\\_model](http://www.nioz.nl/northsea_model).

### 3.3. Hindcast Forcing

The GETM-ERSEM-BFM model was forced using 6 hourly meteorological data provided by the European Centre for Medium-

range Weather Forecasts (ECMWF) ERA 40 and Operational Analysis Hindcasts ([www.ecmwf.int](http://www.ecmwf.int), including pressure, air temperature, wind speed at 10 m height, dew point humidity, and total cloud cover). Spatial edges applied climatological boundary conditions for temperature, salinity, and nutrients. Fresh water discharge and nutrient loads were included for a total of 151 rivers around the model domain, see *Lenhart et al.* [2010] for more details. Direct precipitation was not included. The coupled hydrobiogeochemical model was applied to the North Sea and used to simulate the period 1958–2008, using a spatial resolution of 6 nautical mile and 26 general coordinate layers in the vertical. A previous, multidecadal simulation provided the initial conditions.

### 3.4. Model Validation

Before we analyze the modelled North Sea ecosystem with respect to stratification regimes, we need to ascertain the accuracy of the applied model in representing stratified conditions. To this end, we compared the modeled temperature and salinity with CTD (conductivity-temperature-depth) observations from the ICES database (<http://ocean.ices.dk/>). This database contains a total of 45,324 CTD casts in the period 1980–2008 and within the defined North Sea area (see Figure 1). Figure 2 shows the comparison between observations and modeled results for surface and near-bed temperature, salinity, and density in a normalized Taylor Diagram. For this purpose, all surface and near-bed observations were compared with the closest (temporally and spatially) simulated value, resulting in a correlation coefficient (information regarding phase

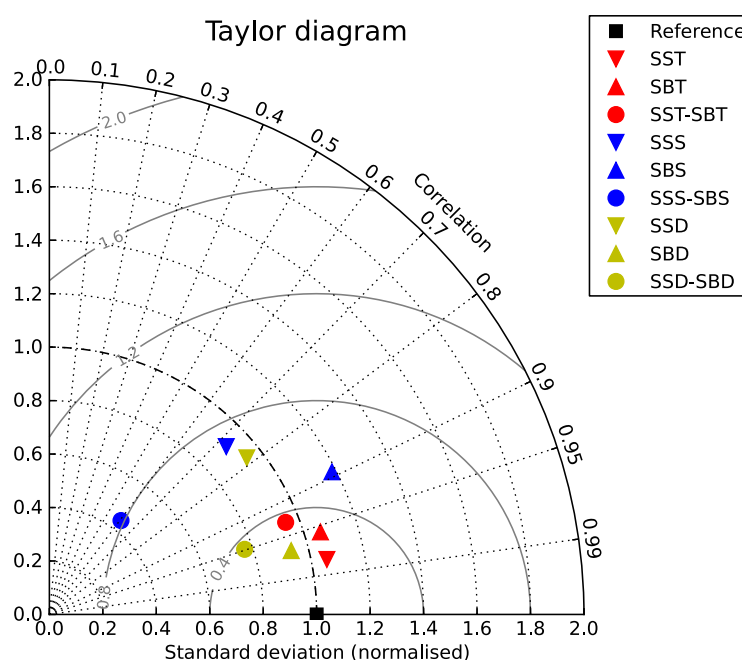


**Figure 2.** Taylor diagram of simulated results versus ICES CTD data covering 1980–2008. The gray internal arcs represent the normalized root-mean square error. SST = sea surface temperature, SBT = sea bed temperature, SSS = sea surface salinity, SBS = sea bed salinity, SSD = sea surface density, and SBD = sea bed density.



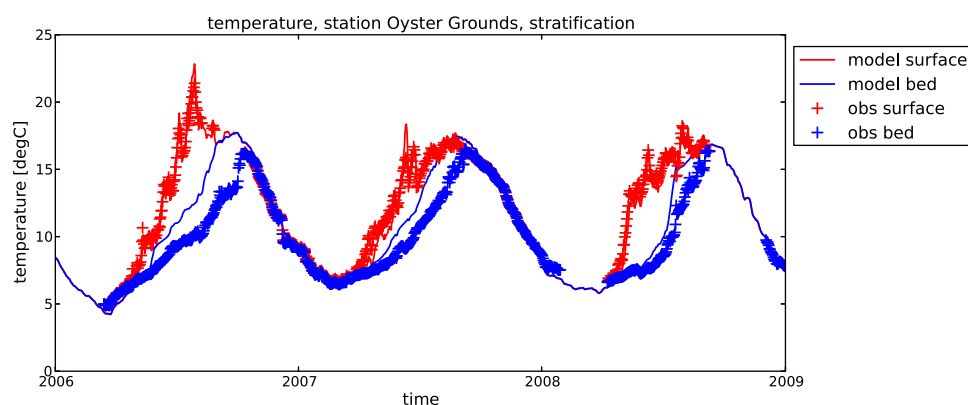


**Figure 3.** Daily comparison of surface and bed observed temperatures and model predictions (both midnight instantaneous values). Observations from the Cefas SmartBuoy in the Oyster Grounds at [54.4°N, 4.02°E].

agreement, shown on the radial axis) and a normalized standard deviation (information regarding amplitude comparison, shown on polar axis). The reference point of (1,0) relates to the situation of the modeled data coinciding exactly with the observational data (correlation of 1, standard deviation equal to observational standard deviation). The diagram also shows the root-mean square-error, as indicated by the grey internal arcs. For more information on Taylor Diagrams, see Jolliff *et al.* [2009]. Simulated temperatures are closer to observed values than simulated salinity values. This is due to the local influence of air temperature and short-wave radiation on sea surface temperature, which is well represented within the GETM model. The main source of error for surface temperature validation lies in the discretization of both the meteorological forcing (6 hourly values at 1.125° spatial resolution) and the models' spatial representation (6 nautical mile grid). Internal diffusive and advective processes transport heat downwards, with necessary model parametrizations leading to a slightly lower correlation and slightly higher root-mean square error for sea bed temperature (with related increased uncertainty in thermo/pycnocline depth and associated biological response). Salinity values are influenced by the simulated general circulation pattern, the applied fresh water forcing, and the spatial resolution of the model, resulting in errors in narrow river plumes and frontal regions. The lack of precipitation and direct land run-off is visible in the lower correlation value for surface salinity compared to sea bed salinity. Comparison of observed water column temperature and salinity differences (SST-SBT and SSS-SBS) shows lower correlation values than the separate comparisons, but still represents a good correlation between simulated and observed values (correlation > 0.6). Validation results for density difference between surface and near-bed waters (on which the subsequent analysis is based) show a correlation of 0.95: we therefore deem the model fit for purpose. The distribution of the used observations covers the whole North Sea and all years (see supporting information Figures S1 and S2).

We also compared simulated stratification with high-frequency (originally 20 min) observations from a single point. SmartBuoy data of surface and sea bed temperatures in the Oyster Grounds (54.4°N, 4.02°E) are shown in Figure 3 with the simulated values for a 3 year period. For more information about SmartBuoy measurements, see Mills *et al.* [2005] and Greenwood *et al.* [2010]. Simulated sea bed temperatures in this location are higher than those observed, causing the model to underpredict stratification duration in the Oyster Grounds. The high near-bed temperatures indicate too much diapycnal exchange of heat within the model at this location. However, interannual variation is large and more high-frequency observations are needed (at different locations) to estimate the models' ability to predict stratification duration.

## 4. Results: Density Stratification Regimes in the North Sea

### 4.1. Definition of Stratified Areas

To determine the homogeneity of the local water column, we consider vertical density stratification. Here, the water column was defined as "stratified" if the density difference between surface (1 m below surface) and near-bed (1 m above sea bed) waters (midnight instantaneous values) exceeded 0.086 kg/m<sup>3</sup> (equivalent of 0.5°C or 0.11 PSU difference in water of 10°C and 34.5 PSU) [Lowe *et al.*, 2009]. Hence, a "mixed" water column may still experience weak stratification. Note that the applied definition allows for ample

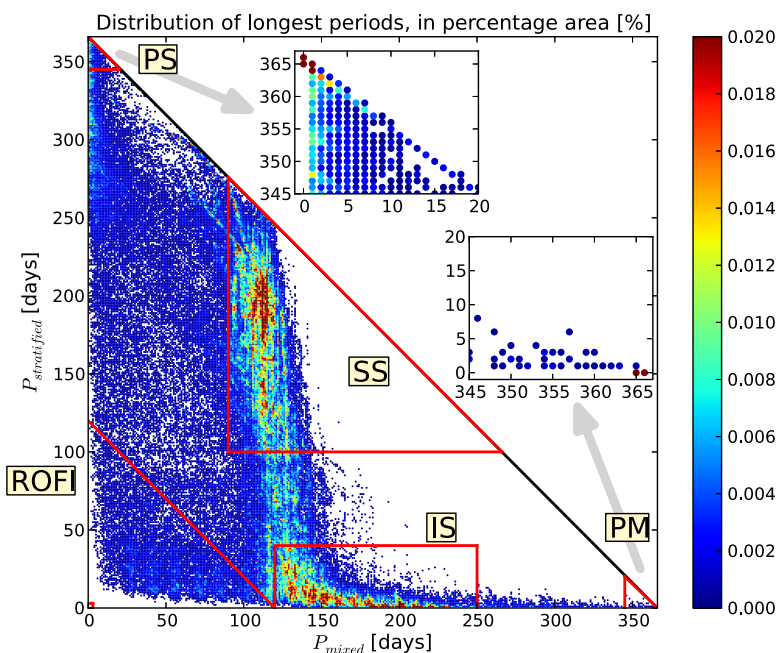


**Figure 4.** Density stratification: distribution of  $P_{mixed}$  and  $P_{stratified}$  with color indicating the average percentage of the North Sea area experiencing the corresponding conditions. The red dots in the subplots represent values beyond the color bar scale: year-round stratified and mixed conditions cover a maximum of 13% and 18% of the North Sea area, respectively. Here PS = permanently stratified, SS = seasonally stratified, IS = intermittently stratified, PM = permanently mixed, and ROFI = Region Of Freshwater Influence.

internal wave breaking, which can lead to episodic injections of nutrients in the surface mixed layer and associated blooms [van Haren et al., 1999]. This mechanism is not included in the model.

In order to define the annual physical conditions of the water column with respect to stratification, we considered two characteristic periods: the longest period of continuous stratified conditions ( $P_{stratified}$ ) and the longest period of continuous mixed conditions ( $P_{mixed}$ ). These periods are deemed indicative of the seasonal chemical and biological cycles that can operate in each area. The hindcast results over the period 1958–2008 were analyzed by determining  $P_{stratified}$  and  $P_{mixed}$  for each spatial model grid point for each year. Figure 4 shows the distribution of  $P_{mixed}$  and  $P_{stratified}$  during the simulated 51 year period, in annually averaged percentage of the North Sea area. Figure 4 shows that not four, but five separate regimes need to be considered. The regimes are indicated in Figure 4 by the red lines and are defined in Table 2. The permanent regimes are shown enlarged in the subplots: these regimes are so permanent that most model grid points fall into the 365 (normal years) and 366 (leap years) category. The area characterized by short-mixed conditions and longer stratified conditions ( $P_{mixed} < 20$ ,  $P_{stratified} > 250$ ) is not considered a separate regime: spatially this regime is only present in a narrow strip adhering to the permanently stratified regime. Separate results for temperature and salinity stratification can be found in supporting information S3 and S4, respectively.

#### 4.2. Distribution of Regimes in the North Sea

Based on the values of longest period of continuous mixed and stratified conditions for each model grid point for each year, we can now visualize the time dominant results spatially. Figure 5 shows the regimes

which occur for the most years in each spatial grid point. The result shows the permanent haline stratification of water in the Norwegian Trench (see also supporting information S4). Outflow from the Baltic Sea is low in salinity (6.0–8.0 PSU compared to North Sea averages of 35.0 PSU), due to its restricted exchange with the North Sea, its high fresh water load and limited evaporation. North Sea circulation forces the Baltic

**Table 2.** Definitions Used for the Different Hydrodynamic Regimes in the North Sea

	$P_{stratified}$ [(days)	$P_{mixed}$ (days)	$P_{stratified} + P_{mixed}$ (days)
Permanently stratified (PS)	> 345	< 20	
Seasonally stratified (SS)	> 120	> 90	
Intermittently stratified (IS)	< 40	$\in [120, 250]$	
Permanently mixed (PM)	< 20	> 345	
Region Of Freshwater Influence (ROFI)	> 3	> 3	< 120

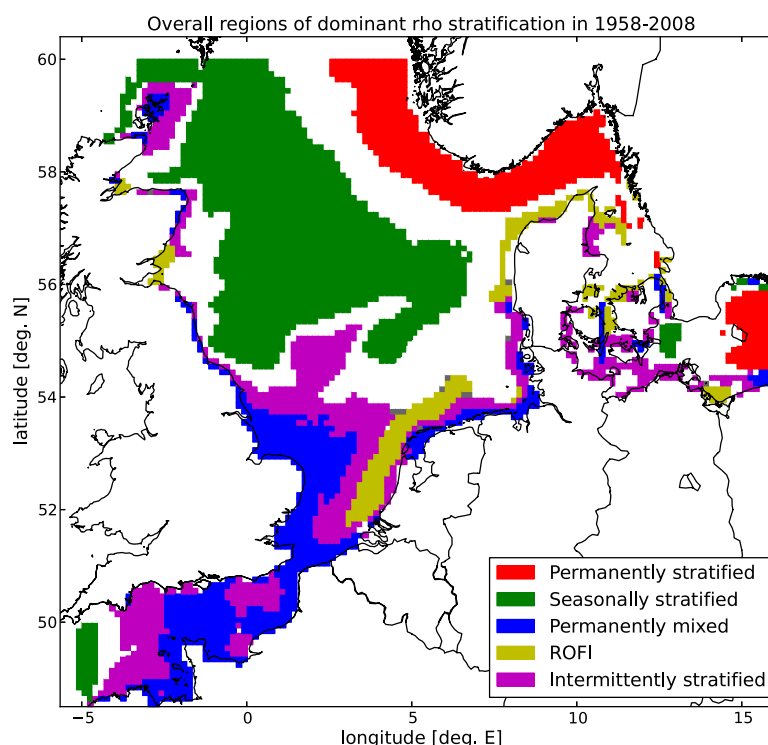


**Figure 5.** Time median results of the modelled, annual regions in the North Sea based on density stratification. Transparent areas indicate areas where the dominant regime occurs for less than 50% of the time (less visible due to minimal occurrence).

outflow to follow the Norwegian coastline until it exits into the North-east Atlantic. The less saline, lighter water from the Baltic overlays the denser, more saline water from the North Sea. As such, this region is permanently stratified due to salinity differences between the top and bottom waters.

The second feature in Figure 5 shows the seasonally stratified area in the northern and central North Sea; this area thermally stratifies in spring (see also supporting information Figure S5) when air temperatures increase, and stays stratified until autumn processes remix the water column. Winter is characterized by continuous mixed conditions.

The third region in Figure 5 is the well-mixed areas in the southern Bight and Channel. Here relatively shallow waters (40 m at most, though some deeper troughs in the channel) are continuously mixed by tidal and wave action and the inflow through the Dover Strait (see also supporting information Figures S5 and S6).

The fourth region identified in Figure 5 is the Regions Of Freshwater Influence, or ROFI's. ROFI's are characterized by a continuous, but seasonally varying, inflow of fresh water, and therefore include estuarine regions and riverine plume areas. The inflow of fresh water into the marine system is opposed by tidal and wave action transporting marine waters into the riverine areas, causing a changing environment of short-lived haline stratification and break up (see also supporting information Figure S6). The influence of Rhine and Meuse freshwater outflow is visible along the Dutch coast line, while Baltic Sea in and outflow combined with local and German Bight riverine inputs results in a ROFI area along the Danish North Sea coast. Note that both the highly variable nature of the German Bight (see supporting material S7) and the applied spatial resolution (6 nautical miles) prevent the occurrence of a more permanent ROFI regime along the German coast line in this simulation.

The fifth region is characterized by long-mixed conditions during winter time and repeated, short-lived thermal stratification in summer. This intermittently stratified region lies adjacent to the permanently mixed region, but is distinctly separate in terms of stratification characteristics (Figure 4).

The location of the tidal mixing front in these results is indicated by the edge of the seasonally stratified regime (using a vertical temperature difference of 0.5°C as indication, as in Holt and Umlauf [2008]). Its variability in time is shown in supporting information video S1, a sequence of Figure 5 for the individual years.



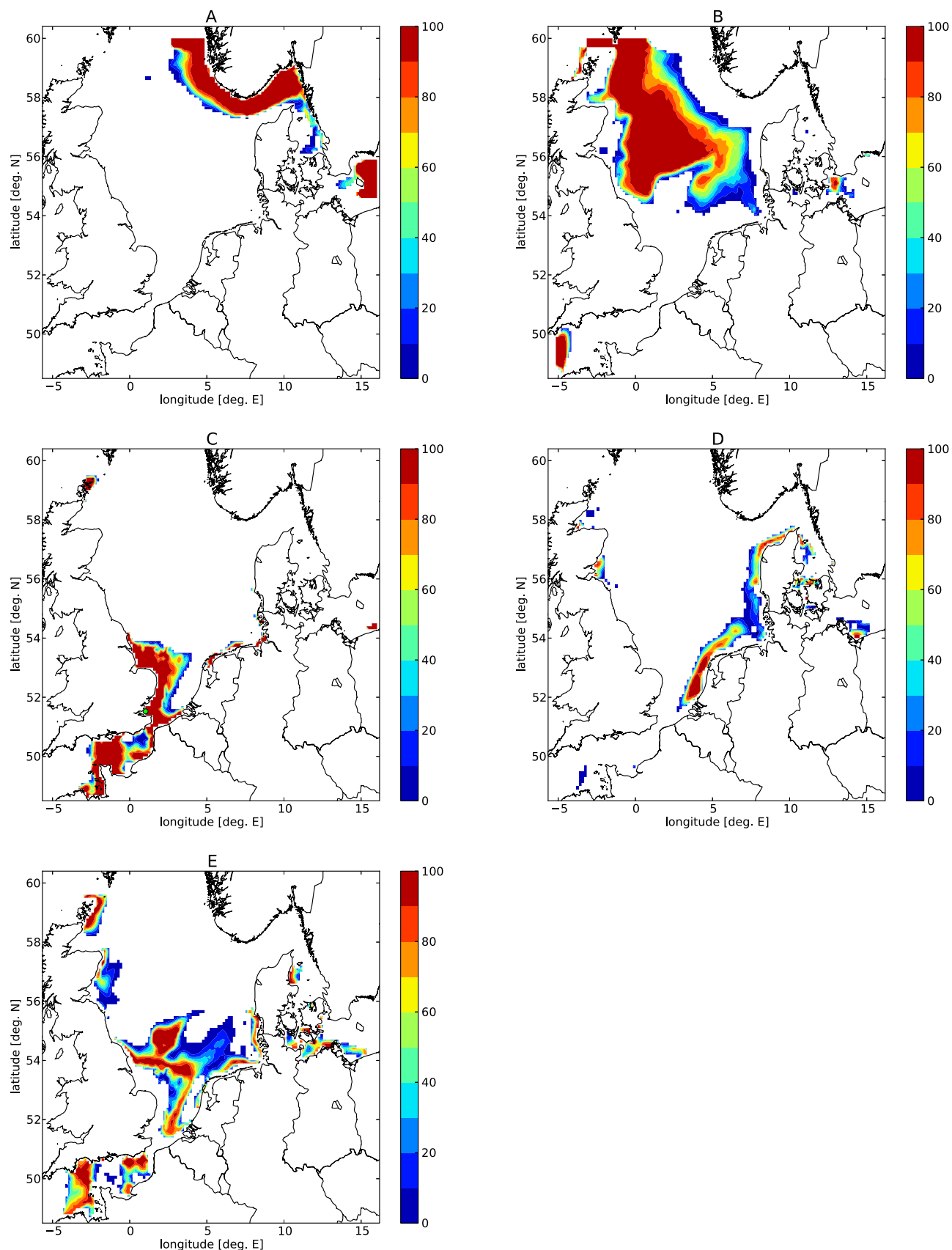


**Figure 6.** Spatial distribution of percentage time spent in each defined regime, over the period 1958–2008. (a) Permanently stratified, (b) seasonally stratified, (c) permanently mixed (the green dot indicates the WARP SmartBuoy location), (d) ROFI, and (e) intermittently stratified.

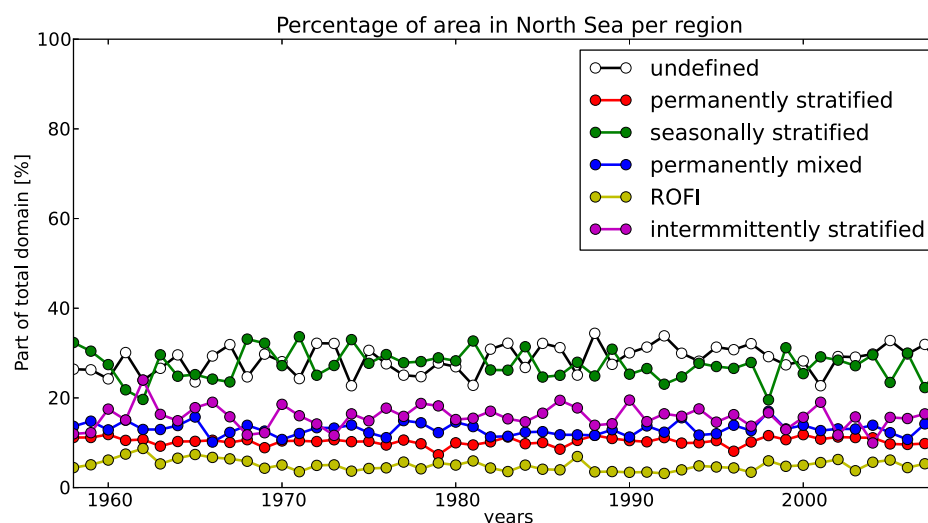


**Figure 7.** Percentage area covered in the North Sea for each regime.

The regions described above are well-known features of the North Sea hydrodynamic regime. All these regions occurred with considerable dominance, well above 50% of the modeled years. However, also of interest are the areas that do not qualify as either one of the five identified regions. These areas are usually characterized by high variability in either (or both) of the duration of continuous mixed and stratified conditions. For example, the location of [54.5° N, 7.0° E] in the German Bight shows  $P_{stratified}$  in the range of 35–140 days a year, while  $P_{mixed}$  has a range of 20–170 days a year. As a result the location qualifies for 12% of the simulated period as being a ROFI area, for another 12% as seasonally stratified and for 2% of the period as intermittently stratified. During the other years, the location is undefined according to Table 2. The Oyster Grounds location used in Figure 3 qualifies as seasonally stratified for 18% of the simulated period, as intermittently stratified for 6% of the time and undefined for the remaining period (see also supporting information S5 for temporal variation in area coverage). To visualize this variability, we look at the percentage of time any area can be defined according to Table 2, as shown in Figure 5. The results, shown in Figure 6, indicate that the permanently stratified and permanently mixed areas are well defined: the transitional area in both cases is small. Seasonally stratified, intermittently stratified, and ROFI areas are much more variable. The seasonally stratified area shows the extension into the German Bight associated with a south-east shift of the tidal mixing front (following the Elbe Channel, see also supporting information S7), caused by above average air temperatures and below average riverine outflow and wind conditions. In the same way, the intermittently stratified area extends northwards in opposite years, characterized by higher wind speeds and lower air temperatures. ROFI areas extend in years of high rainfall and associated fresh water run-off. The Elbe channel in the German Bight serves as a pathway for extension of the seasonally stratified area south-eastwards, causing an interruption of the ROFI area along the continental coast following the Rhine and Meuse outflows.

Figure 7 shows that, on average, 71% of the North Sea area falls in the defined categories. In a 51 year average, 10% of the North Sea can be classified as permanently stratified, 27% as seasonally stratified, 16% as intermittently stratified, 13% as permanently mixed, and 5% as ROFI. This means that 29% of the North Sea area is undefined according to Table 2, on average. The annual area covered by each stratified region shows no significant trend over the hindcast period (note that oceanic influences are limited due to climatological boundary conditions). However, annual differences do occur and spatial coverage may vary even if total area does not (see supporting information S7).

## 5. Results: Biological Consequences

The pelagic regimes identified in the previous section and shown in Figure 5 can be seen as a physical extension of the work by *Pingree and Griffiths* [1978]. The ERSEM-BFM model allows simulation of the

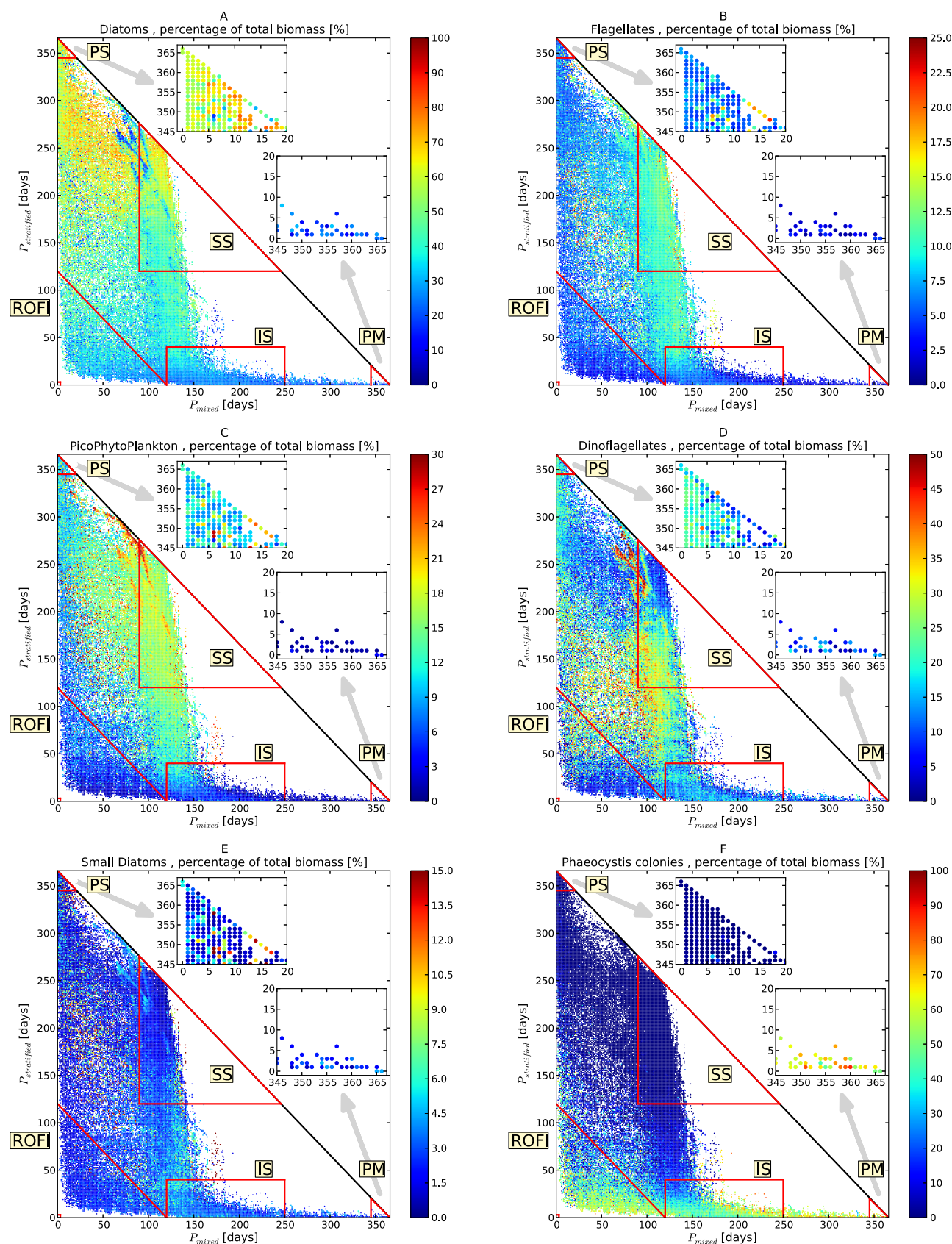


**Figure 8.** Distribution of phytoplankton with respect to the different regimes, in percentage of total biomass. (a) Diatoms, (b) flagellates, (c) picophytoplankton, (d) dinoflagellates, (e) small diatoms, and (f) *Phaeocystis*.

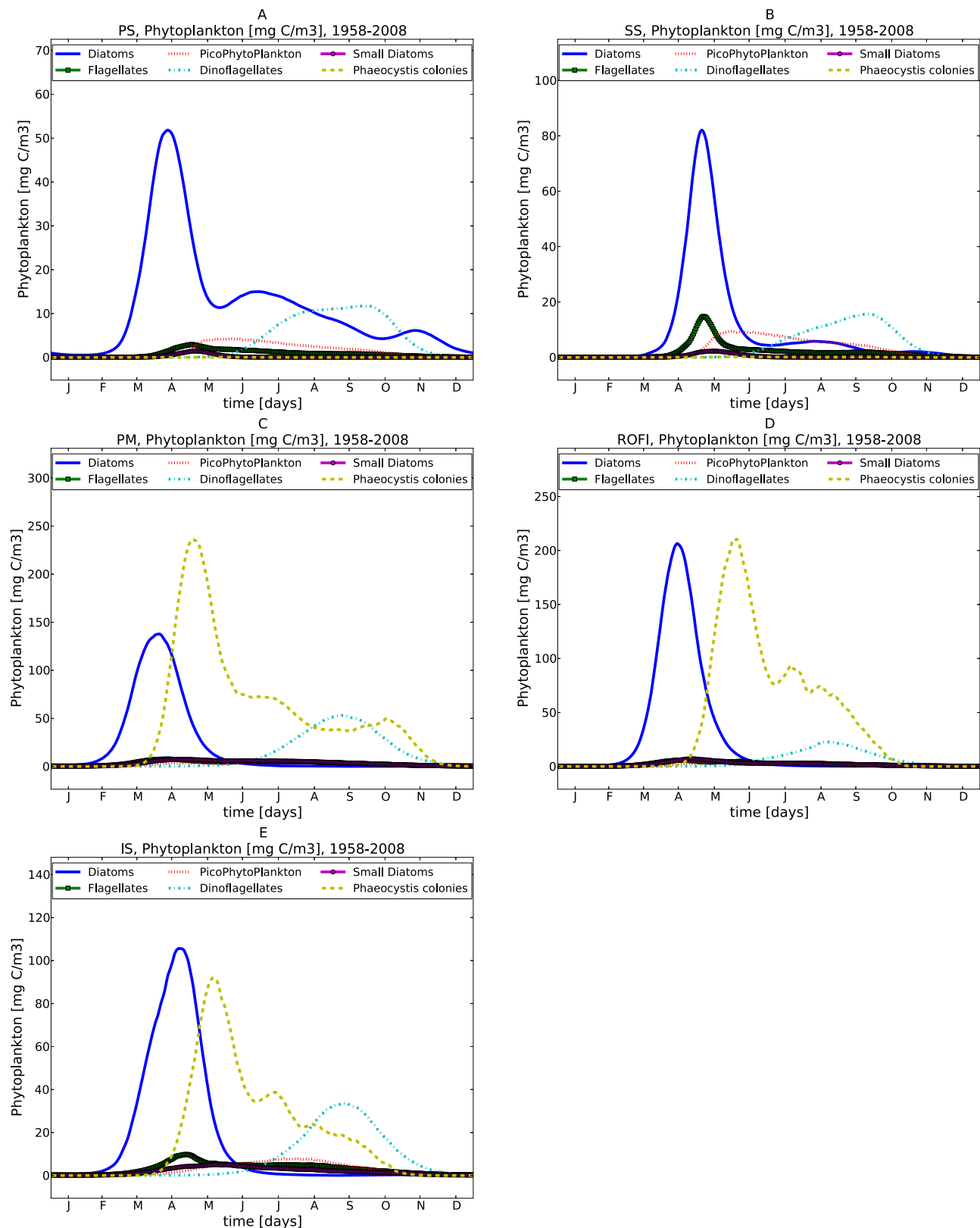


**Figure 9.** Annual mean phytoplankton dynamics for the five different regimes. Mean (1958–2008) seasonal cycle based on spatially and depth-averaged values for the ERSEM-BFM phytoplankton groups for the largest polygon in each regime. (a) Permanently stratified area (Norwegian trench), (b) seasonally stratified area (central and northern North Sea), (c) permanently mixed area (Southern Bight), (d) ROFI area (Rhine plume), and (e) intermittently stratified area (central North Sea).

biological response to the physical processes in these regimes. Biological activity is mainly driven by light and nutrient availability, and both depend on local physical conditions: stratification can limit nutrient access and turbulent mixing can cause increased levels of suspended particulate matter, affecting light attenuation [see *van Haren et al.*, 1998, for a detailed analysis of the start of the spring bloom in the seasonally stratified North Sea]. These processes directly affect the depth level of phytoplankton and the total number of photons received by a microalgal cell in 24 h *Tett* [1987]. The applied model includes a simple formulation for local resuspension by waves, see *van der Molen et al.* [2014] for details.

Because the biological model has not been validated to the same extent as the physical model, these simulated biological consequences should be considered tentative, and this section also includes some discussion of their reliability.

For each year, for each spatial model grid point, we determined the total (vertically integrated) phytoplankton biomass and the percentage contribution from each functional group. Note that modeled phytoplankton biomass represent instantaneous values at midnight (for each vertical layer). Figure 8 shows the averaged contributions for the six phytoplankton functional groups of Table 1 as a function of the physical parameters  $P_{stratified}$  and  $P_{mixed}$ . Three main patterns can be distinguished in these model results:

1. Areas with prolonged stratification ( $> 160$  days) are characterized by predominantly diatom biomass.
2. Areas which experience seasonal stratification exhibit the largest contributions from flagellates and picophytoplankton, though diatom biomass still dominates. This may be due to the location of the seasonally stratified area, which is far removed from anthropogenic nutrients sources, favoring organisms with a large surface/volume ratio.
3. Areas with mixed conditions show biomass dominance of the colonial alga *Phaeocystis*, enhanced by nutrient enrichment in the southern North Sea. *Phaeocystis* becomes dominant once silica limitation reduces diatom abundance.

Figure 9 shows the simulated annual signal of the six phytoplankton functional groups of Table 1 in four areas that are the largest units of the regime types PS, SS, PM, and ROFI. Each of these regime types shows a distinct pattern in terms of timing and the succession of lifeforms.

All areas exhibit strong diatom-based spring blooms. In stratified areas, diatoms are succeeded by thermocline based flagellates and upper mixed layer picophytoplankton, followed by dinoflagellates in late summer and early autumn (see also *van Leeuwen et al.* [2013]). In contrast, in high energy, turbulent regions like the permanently mixed and ROFI areas the diatom spring bloom is followed by a long period of abundance of *Phaeocystis*, with a late summer increase in dinoflagellate levels.

While the SS regime demonstrates the “classical” temperate cycle of phytoplankton, with a spring diatom bloom peaking in May and an early autumn growth of dinoflagellates, a broadly similar cycle in the PS regime starts earlier (peaking in April), finishes later, and maintains greater abundance of diatoms throughout the summer.

The distinction between the PS+SS and the PM+ROFI regimes broadly corresponds to that made by *Rodhe et al.* [2006] between the ecosystems of the “seasonally stratified north and central North Sea” and those of its “southern and western coastal regions” below the main tidal mixing front at about 55°N. Evidence for a longer productive season in haline-stratified waters is provided for example from Scottish west-coast (fjordic) sea-lochs such as Creran [*Tett and Wallis*, 1978] and Striven [*Tett et al.*, 1986]. Deep chlorophyll maxima have been observed in the central stratified North Sea [*Richardson et al.*, 2000; *Weston et al.*, 2005; *Fernand et al.*, 2013], although mixed layer depths may preclude them from northern stratified waters [*Tett and Lee*, 2005] (*van Haren et al.* [2003] shows chlorophyll presence throughout the surface mixed layer, as a result of mixing events resuspending near-pycnocline phytoplankton). Late-spring blooms of *Phaeocystis* are well documented in the nutrient-enriched mixed waters and ROFIs of the southern North Sea [*Lancelot et al.*, 1987; *Gieskes et al.*, 2007; *Gypens et al.*, 2007].

Spatially extensive observations in the southern and central North Sea made at least monthly in 1988/1989 *Howarth et al.* [1993]; *Joint and Pomroy* [1993]; *Mills et al.* [1994]; and *Tett et al.* [1993] confirm the “classical” phytoplankton cycle in seasonally stratifying waters, with the bloom peaking just after the onset of thermal stratification. In the southern and western mixed and ROFI waters, the Spring bloom started between March and May, depending on mixed-layer optical thickness, and often included abundant *Phaeocystis*. Thereafter



patterns of biomass change were varied, depending on location. Thus we may conclude that the comparative picture of seasonal succession shown by the simulations in Figure 9 is broadly correct for the larger life-forms of diatoms, dinoflagellates, and *Phaeocystis*. There is very little published quantitative information with which to compare the simulated time series of the smaller phytoplankters.

## 6. Discussion

Progress in understanding the oceanography of shelf seas has come about through a combination of observation and theory. It is notable that the development of remote sensing of sea-surface temperature stimulated the formulation of the  $h/u^3$  model by Simpson and Hunter and to the observation during research cruises of the physics and biology of tidal mixing fronts [Pingree *et al.*, 1975; Simpson *et al.*, 1979]. As already noted, this provided the impetus for the influential model of Pingree and Griffiths [1978], and thus, several model generations later, to the GETM-ERSEM-BFM model used in the present work.

In the present age of austerity, however, the time of research ships has become scarce, and it is no longer possible to make regular maps of physical and biological properties on a sufficiently large scale to be useful for understanding the current state of UK shelf-sea ecosystems (c.f. Pingree *et al.* [1978]; Howarth *et al.* [1993]). Ships of opportunity, including those towing Continuous Plankton Recorders (CPR) Gieskes *et al.* [2007]; Richardson *et al.* [2006] can contribute useful observations of some properties, as can remote sensing [e.g., Astoreca *et al.*, 2009] even if the latter is hindered by cloud cover and interpretational difficulties in optical case II waters. Well-equipped moorings, such as the Cefas SmartBuoys [Mills *et al.*, 2005] can provide intensive time-series at fixed sites: the challenge is to ensure that these sites are representative. A similar challenge also applies to CPR routes.

The present generation of numerical models—especially hydrodynamic models such as GETM—provide part of the answer. They can provide both the high spatial resolution and the extension in space and time that was needed for the analysis presented in this paper. Thus, the 51 year modeled hindcast has provided us with a solid foundation for the identification and classification of stratification regimes in the North Sea, and the resulting mapping can provide a guide for the placement of scarce resources such as moorings.

Of course, models do not provide the last word on the topic, or, at least, not until they have been verified by observations more detailed than those presented here (e.g., by detailed observation of stratification-related processes as those presented in van Haren *et al.* [1997, 1998, 2003], as the model indicated too much diffusive heat exchange across the pycnocline (Figure 3)). This is especially true with respect to the biological results, which should be considered as no more than an indication of the sort of biotic differences to be expected amongst the identified hydrodynamic regimes. Indeed, both observations such as Tett *et al.* [1993] and simulations (Figure 9) suggest that within the North Sea marine biomes may be differentiated not by the main primary producer, but by the relative contribution and succession of different primary producers.

As already mentioned, the model results can also be used to identify where new observations are required in order to improve understanding of marine ecosystem dynamics and for monitoring required to meet the needs of a range of different policy drivers including the Marine Strategy Framework Directive (MSFD). In general, the results from the simulations illustrate the strong variability of shelf-seas marine ecosystems in space and time. There are some important implications of the results of this work for current and future monitoring and assessment of environmental status as required by a range of European policy drivers including the MSFD.

For example, a key question that concerns the effectiveness of current marine monitoring programmes is the extent to which sampling stations are representative of wider regions. Cefas SmartBuoys [Mills *et al.*, 2005] make high-frequency (20 min) measurements at fixed locations around the coast of the UK including the Thames estuary (permanently mixed region). The mooring site is marked in Figure 5c and falls within the near-permanent core of this region, which suggests that the SmartBuoy observations should be representative of this ecohydrodynamic region.

Such considerations can play an important part in the design of future monitoring programmes. In particular, they point to the need to obtain time series of key physical, biological, chemical, and optical properties at a small set of sentinel sites located in the persistent cores of each of the ecohydrodynamic regions in the

management unit that the MSFD names the “Greater North Sea.” There is an equivalent need in the MSFD’s “Celtic Seas,” to the west of Britain. Because nutrient enrichment and the indirect effects of fishing are crucial but somewhat localized pressures, it is desirable that some sites be duplicated in areas of high and low pressure, for example in the nutrient-rich Rhine-mouth and nutrient-poor Moray Firth (Scotland) ROFIs.

Finally, there is a need to observe and analyze plankton in relation to hydrodynamics over a number of years in at least one part of the Greater North Sea that is mapped as undefined in our study. This should help determine whether the pelagic biome is a within-year response to the hydrodynamic regime, or an equilibrium response that requires inputs of seed organisms from other regions and takes a number of years to develop the appropriate biome. Until we can answer this question, it will be necessary to be cautious in interpreting water quality data from these regions, which may potentially vary between two or perhaps three biomes over the course of several years, and which occupy about 29% of the North Sea.

## 7. Conclusions

In this article, we have identified distinct physical regimes in the North Sea based on density stratification characteristics. Modeled results presented here have shown the existence of five hydrodynamic regimes in the North Sea: permanently stratified, seasonally stratified, intermittently stratified, permanently mixed, and ROFI (Region Of Freshwater Influence). These regimes form spatially and temporally stable features of the North Sea hydrodynamic regime, with the core areas covering 71% of the total North Sea domain (Figures 5–7). The remaining 29% is characterized by large interannual variability which defies classification. These are mainly transitional areas, which can belong to different regimes in different years.

We have made some progress in showing how the floristic composition of the phytoplankton (as shown in the contribution and seasonality of each simulated lifeform) relates to physical regime, but there remains much more to do both with simulations and with observations to assemble the definitive account of links between physics and biology that will correspond to the picture painted by biome theory of terrestrial environments. Nevertheless, effective marine management, such as that required by the MSFD, must take account of the existence of five ecohydrodynamic regimes in the North Sea, and their likely biological consequences, as well as acknowledging the large interannual variability in the zones between the regime cores.

## Acknowledgments

This work was enabled through Defra projects ME5302 (Ecosystem Health) and C5935 (Meeting the needs of MSFD monitoring) and the DEVOTES project (Development of innovative tools for understanding marine biodiversity and assessing good Environmental Status), funded by the EU FP7 (grant agreement 308392). The lead author also thanks ERSEM-BFM expert Piet Ruardij (NIOZ, the Netherlands) for the many fruitful discussions, Rodney Forster and David Stephens (Cefas) for GIS support and two anonymous reviewers for the very detailed comments (which considerably improved the manuscript). Observations used were obtained from the ICES database (available at <http://ocean.ices.dk/>, salinity and temperature data) and from Cefas Smartbuoy (available at <http://cefasmapping.defra.gov.uk/Smartbuoy/Map>, temperature data).

## References

- Astoreca, R., V. Rousseau, K. Ruddick, C. Knechciak, B. Van Mol, J. Y. Parent, and C. Lancelot (2009), Development and application of an algorithm for detecting *Phaeocystis globosa* blooms in the case 2 southern north sea waters, *J. Plankton Res.*, 31(3), 287–300, doi:10.1093/plankt/fbn116.
- Baretta, J. W., W. Ebenhö, and P. Ruardij (1995), The European Regional Seas Ecosystem Model: A complex marine ecosystem model, *J. Mar. Res.*, 33, 233–246.
- Burchard, H., and K. Bolding (2002), Getm: A general estuarine transport model, Institute for Environment and Sustainability, Joint Research Centre Ispra Tech. Rep. EUR 20253 EN, Eur. Comm.
- Clements, F. E. (1916), *Plant Succession: An Analysis of the Development of Vegetation*, Publ. No. 242, 658 pp., Carnegie Inst. of Wash., Baltimore, USA.
- Clements, F. E. (1936), Nature and structure of the climax, *J. Ecol.*, 24(1), 252–284.
- Fernand, L., T. Morris, K. Weston, N. Greenwood, J. Brown, and T. Jickells (2013), The contribution of the deep chlorophyll maximum to primary production in a seasonally stratified shelf sea, the North Sea, *Biogeochemistry*, 113(1–3), 153–166.
- Gieskes, W. W. C., S. C. Leterne, H. Peletier, M. Edwards, and P. C. Reid (2007), *Phaeocystis* colony distribution in the north Atlantic ocean since 1948, and interpretation of long-term changes in the *phaeocystis* hotspot in the north sea, *Biogeochemistry*, 83(1), 49–60, doi: 10.1007/s10533-007-9082-6.
- Greenwood, N., et al. (2010), Detection of low bottom water oxygen concentrations in the north sea; implications for monitoring and assessment of ecosystem health, *Biogeosciences*, 7, 1357–1373, doi:10.5194/bg-7-1357-2010.
- Gypens, N., G. Lacroix, and C. Lancelot (2007), Causes of variability in diatom and *phaeocystis* blooms in Belgian coastal waters between 1989 and 2003: A model study, *J. Sea Res.*, 57(1), 19–35, doi:10.1016/j.seares.2006.07.004.
- Hardy, A. C. (1956), *The Open Sea – It's Natural History: The World of Plankton*, 103 pp., Collins, London, U. K.
- Hofmeister, R., H. Burchard, and J.-M. Beckers (2010), Non-uniform adaptive vertical grids for 3D numerical ocean models, *Ocean Modell.*, 33, 70–86, doi:10.1016/j.ocemod.2009.12.003.
- Hofmeister, R., J.-M. Beckers, and H. Burchard (2011), Realistic modelling of the exceptional inflows into the central Baltic Sea in 2003 using terrain-following coordinates, *Ocean Modell.*, 39, 233–247, doi:10.1016/j.ocemod.2011.04.007.
- Holt, J., and L. Umlauf (2008), Modelling the tidal mixing fronts and seasonal stratification of the northwest European continental shelf, *Cont. Shelf Res.*, 28(7), 887–903, doi:10.1016/j.csr.2008.01.012.
- Holt, M., Z. Li, and J. Osborne (2003), Real-time forecast modelling for the NW European shelf seas, *Elsevier Oceanogr. Ser.*, 69, 484–489, doi: 10.1016/S0422-9894(03)80076-4.
- Howarth, M. J., et al. (1993), Seasonal cycles and their spatial variability, *Philos. Trans. R. Soc. London A*, 343, 383–403.

- Joint, I., and A. Pomroy (1993), Phytoplankton biomass and production in the southern north sea, *Mar. Ecol. Prog. Ser.*, **99**, 169–182.
- Jolliff, J. K., J. C. Kindle, I. Shulman, B. Penta, M. A. Friedrichs, R. Helber, and R. A. Arnone (2009), Summary diagrams for coupled hydrodynamic-ecosystem model skill assessment, *J. Mar. Syst.*, **76**(12), 64–82, doi:10.1016/j.jmarsys.2008.05.014.
- Kühn, W., J. Pätsch, H. Thomas, A. V. Borges, L.-S. Schiettecatte, Y. Bozec, and A. E. F. Prowe (2010), Nitrogen and carbon cycling in the North Sea and exchange with the North AtlanticA model study, Part II: Carbon budget and fluxes, *Cont. Shelf Res.*, **30**(16), 1701–1716, doi:10.1016/j.csr.2010.07.001.
- Lancelot, C., G. Billen, A. Sournia, T. Weisse, F. Colijn, M. J. W. Veldhuis, A. Davies, and P. Wassman (1987), Phaeocystis blooms and nutrient enrichment in the continental coastal zones of the North Sea, *Ambio*, **16**, 38–46.
- Legendre, L., and F. Rassoulzadegan (1995), Plankton and nutrient dynamics in marine waters, *Ophelia*, **41**, 153–172.
- Legendre, L., and F. Rassoulzadegan (1996), Food-web mediated export of biogenic carbon in oceans: Environmental control, *Mar. Ecol. Prog. Ser.*, **145**, 179–193.
- Lenhart, H.-J., D. K. Mills, J. G. Baretta-Bekker, S. M. Van Leeuwen, J. Van der Molen, and J. W. B. et al. (2010), Predicting the consequences of nutrient reduction on the eutrophication status of the North Sea, *J. Mar. Syst.*, **81**, 148–170, doi:10.1016/j.jmarsys.2009.12.014.
- LeQuéré, C., et al. (2005), Ecosystem dynamics based on plankton functional types for global ocean biogeochemistry models, *Global Change Biol.*, **11**, 2016–2040, doi:10.1111/j.1365-2486.2005.01004.x.
- Lowe, J. A., et al. (2009), UK Climate Projections science report: Marine and coastal projections, technical report, 99 pp., Met Off. Hadley Cent., Exeter, U. K.
- Margalef, R. (1978), Life-forms of phytoplankton as survival alternatives in an unstable environment, *Oceanol. Acta*, **1**, 493–509.
- Mills, D. K., P. Tett, and G. Novarino (1994), The spring bloom in the south-western north sea in 1989, *Netherlands J. Sea Res.*, **33**, 65–80.
- Mills, D. K., N. Greenwood, S. Kröger, M. Devlin, D. B. Sivy, D. B. Pearce, S. Cutchey, and S. J. Malcolm (2005), New approaches to improve the detection of eutrophication in UK coastal waters, *Environ. Res. Eng. Manage.*, **2**(32), 36–42.
- Mork, M. (1981), Circulation phenomena and frontal dynamics of the Norwegian coastal current, *Philos. Trans. R. Soc. London A*, **302**, 634–648.
- Odum, E. P., and G. W. Barrett (2005), *Fundamentals of Ecology*, 5th ed., 598 pp., Thomson Brooks/Cole, Belmont, Calif.
- Pingree, R. D., and D. K. Griffiths (1978), Tidal fronts on the shelf seas around the British isles, *J. Geophys. Res.*, **83**(C9), 4615–4622, doi:10.1029/JC083iC09p04615.
- Pingree, R. D., P. R. Pugh, P. M. Holligan, and G. R. Forster (1975), Summer phytoplankton blooms and red tides along tidal fronts in the approaches to the English channel, *Nature*, **258**, 672–677, doi:10.1038/258672a0.
- Pingree, R. D., P. M. Holligan, and G. T. Mardell (1978), The effects of vertical stability on phytoplankton distributions in the summer on the northwest European shelf, *Deep Sea Res.*, **25**(C9), 1011–1028, doi:10.1016/0146-6291(78)90584-2.
- Reynolds, C. S. (1989), *Physical Determinants of Phytoplankton Succession*, pp. 9–56, Springer, Madison, Wis.
- Reynolds, C. S., V. Huszar, C. Kruk, L. Naselli-Flores, and S. Melo (2002), Towards a functional classification of the freshwater phytoplankton, *J. Plankton Res.*, **24**(5), 417–428, doi:10.1093/plankt/24.5.417.
- Richardson, A. J., A. W. Walne, A. W. G. John, T. D. Jonas, J. A. Lindley, D. W. Sims, D. Stevens, and M. Witte (2006), Using continuous plankton recorder data, *Prog. Oceanogr.*, **68**(1), 27–74, doi:10.1016/j.pocean.2005.09.011.
- Richardson, K., A. W. Visser, and F. B. Pedersen (2000), Subsurface phytoplankton blooms fuel pelagic production in the North Sea, *J. Plankton Res.*, **22**, 1663–1671.
- Ricklefs, R. E., J. B. Losos, and T. M. Townsend (2007), Evolutionary diversification of clades of squamate reptiles, *J. Evol. Biol.*, **20**(5), 1751–1762, doi:10.1111/j.1420-9101.2007.01388.x.
- Rodhe, J., P. Tett, and F. Wulff (2006), Chapter 26: The Baltic and north seas: A regional review of some important physical-chemical-biological interaction processes, in *The Sea, Volume 14B, The Global Coastal Ocean: Interdisciplinary Regional Studies and Syntheses: The Coasts of Africa, Europe, Middle East, Oceania and Polar Regions*, edited by A. R. Robinson and K. Brink, pp. 1033–1075, Harvard Univ. Press, Cambridge, Mass.
- Russell, F. S. (1939), Hydrographical and biological conditions in the north sea as indicated by plankton organisms, *J. Cons. Cons. Int. Explor. Mer.*, **XIV**(2), 171–192.
- Siddorn, J., J. Allen, J. Blackford, F. Gilbert, J. Holt, M. Holt, J. Orborne, R. Proctor, and D. Mills (2007), Modelling the hydrodynamics and ecosystem of the north-west European continental shelf for operational oceanography, *J. Mar. Syst.*, **65**(1–4), 417–429, doi:10.1016/j.jmarsys.2006.01.018.
- Simpson, J. H. (1997), Physical processes in the Rof regime, *J. Mar. Syst.*, **12**(1–4), 3–15, doi:10.1016/S0924-7963(96)00085-1.
- Simpson, J. H., and J. R. Hunter (1974), Fronts in the Irish sea, *Nature*, **250**, 404–406, doi:10.1038/250404a0.
- Simpson, J. H., and T. P. Rippeth (1993), The clyde sea: A model of the seasonal cycle of stratification and mixing, *Estuarine, Coastal Shelf Sci.*, **37**(2), 129–144, doi:10.1006/ecss.1993.1047.
- Simpson, J. H., D. J. Edelsten, A. Edwards, N. G. C. Morris, and P. B. Tett (1979), The islay front: Physical structure and phytoplankton distribution, *Estuarine Coastal Mar. Sci.*, **9**, 713–726, doi:10.1016/S0302-3524(79)80005-5.
- Smayda, T. J., and C. S. Reynolds (2001), Community assembly in marine phytoplankton: Application of recent models to harmful dinoflagellate blooms, *J. Plankton Res.*, **23**(5), 447–461, doi:10.1093/plankt/23.5.447.
- Smith, R. (1992), *Elements of Ecology*, 3rd ed., Harper Collins, N. Y.
- Stips, A., K. Bolding, T. Pohlman, and H. Burchard (2004), Simulating the temporal and spatial dynamics of the north sea using the new model GETM (general estuarine transport model), *Ocean Dyn.*, **54**, 266–283.
- Tett, P. (1987), Modelling the growth and distribution of marine microplankton, *Soc. Gen. Microbiol. Symp.*, **41**, 387–425.
- Tett, P., and A. Edwards (1984), Mixing and plankton: An interdisciplinary theme in oceanography, *Oceanogr. Mar. Biol.*, **22**, 99–123.
- Tett, P., and J.-Y. Lee (2005), Nsi ratios and the “balance of organisms”: Prowqm simulations of the northern north sea, *J. Sea Res.*, **54**, 70–91, doi:10.1016/j.seares.2005.02.012.
- Tett, P., and A. Wallis (1978), The general annual cycle of chlorophyll standing crop in loch Creran, *J. Ecol.*, **66**, 227–239.
- Tett, P., R. Gowen, B. Grantham, J. Jones, and B. Miller (1986), The phytoplankton ecology of the firth of clyde sea-lochs striven and fyne, *Proc. R. Soc. Edinburgh*, **90B**, 223–238, doi:10.1017/S026972700005005.
- Tett, P., et al. (1993), Biological consequences of tidal stirring gradients in the north sea, *Philos. Trans. R. Soc. London A*, **343**(1669), 493–508, doi:10.1098/rsta.1993.0061.
- Tett, P., et al. (2007), Defining and detecting undesirable disturbance in the context of eutrophication, *Mar. Pollut. Bull.*, **55**(1–6), 282–297, doi:10.1016/j.marpolbul.2006.08.028.

- van der Molen, J., J. N. Aldridge, C. Coughlan, E. R. Parker, D. Stephens, and P. Ruardij (2013), Modelling marine ecosystem response to climate change and trawling in the North Sea, *Biogeochemistry*, *113*, 1–24, doi:10.1007/s10533-012-9763-7.
- van der Molen, J., H. C. M. Smith, P. Lepper, S. Limpenny, and J. Rees (2014), Predicting the large-scale consequences of offshore wind turbine array development on a north sea ecosystem, *Cont. Shelf Res.*, *85*, 60–72, doi:10.1016/j.csr.2014.05.018.
- van Haren, H., P. Ruardij, H. Ridderinkhof, and D. Mills (1997), The integrated north sea programme (INP), in *Operational Oceanography, the Challenge for European Cooperation, Proceedings of the First International Conference on EuroGOOS*, edited by J. H. S. et al., pp. 529–538, Elsevier, Amsterdam, doi:10.1016/S0422-9894(97)80064-5.
- van Haren, H., D. K. Mills, and L. P. M. J. Wetsteyn (1998), Detailed observations of the phytoplankton spring bloom in the stratifying central north sea, *J. Mar. Res.*, *56*, 655–680, doi:10.1357/002224098765213621.
- van Haren, H., L. Maas, J. T. F. Zimmerman, H. Ridderinkhof and H. Malschaert, (1999), Strong inertial currents and marginal internal wave stability in the central North Sea, *Geophys. Res. Lett.*, *26*, 2993–2996, doi:10.1029/1999GL002352.
- van Haren, H., M. J. Howarth, K. Jones, and I. Ezzi (2003), Autumnal reduction of stratification in the northern north sea and its impact, *Cont. Shelf Res.*, *23*, 177–191, doi:10.1016/S0278-4343(02)00171-1.
- van Leeuwen, S. M., J. van der Molen, P. Ruardij, L. Fernand, and T. Jickells (2013), Modelling the contribution of deep chlorophyll maxima to annual primary production in the North Sea, *Biogeochemistry*, *113*, 137–152, doi:10.1007/s10533-012-9704-5.
- Verspecht, F., T. Rippeth, M. Howarth, A. Souza, J. Simpson, and H. Burchard (2009), Processes impacting on stratification in a region of freshwater influence: Application to liverpool bay, *J. Geophys. Res.*, *114*, C11022, doi:10.1029/2009JC005475.
- Wakelin, S., J. Holt, J. Blackford, J. Allen, M. Butenschön, and Y. Artioli (2012), Modeling the carbon fluxes of the northwest European continental shelf: Validation and budgets, *J. Geophys. Res.*, *117*, C05020, doi:10.1029/2011JC007402.
- Weston, K., L. Fernand, D. K. Mills, R. Delahunty, and J. Brown (2005), Primary production in the deep chlorophyll maximum of the central North Sea, *J. Plankton Res.*, *27*(9), 909–922, doi:10.1093/plankt/fbi064.
- Williams, R., and J. Lindley (1980), Plankton of the Fladen ground during flex 76 i. spring development of the plankton community, *Mar. Biol.*, *57*(2), 73–78, doi:10.1007/BF00387372.